

Direct mechanochemical synthesis and characterization of SrWO₄ nanoparticles

M. Gancheva^{1*}, R. Iordanova¹, L. Mihailov²

¹*Institute of General and Inorganic Chemistry, Bulgarian Academy of Sciences, Acad. G. Bonchev str., bl.11, 1113 Sofia, Bulgaria*

²*Faculty of Chemistry and Pharmacy, Sofia University "St. Kliment Ohridski", J. Bourchier blvd 1, 1164 Sofia, Bulgaria*

Received: September 14, 2022; Revised: November 16, 2022

Single-phase nanocrystalline SrWO₄ was successfully synthesized by direct mechanochemical reaction at room temperature. A stoichiometric mixture of SrCO₃ and WO₃ in a 1:1 molar ratio was subjected to intense mechanical treatment in air using a planetary ball mill at different ball-to-powder weight ratios (BPR). The phases and structural transformations were monitored by X-ray diffraction (XRD) and infrared (IR) spectroscopy. Morphology of the obtained products was determined by transmission electron microscopy (TEM). The synthesis of SrWO₄ occurred after 1 h milling time at a high ball-to-powder weight ratio (20:1) and a milling speed of 500 rpm. On the other hand, the SrWO₄ formation was completed after 4 h milling time at a lower ball-to-powder weight ratio (10:1) and the same milling speed. The average particle size of the as-prepared SrWO₄ powders was found to be 21 nm which decreased to 16 nm on increasing the ball-to-powder weight ratio (20:1). The UV-Vis absorption spectra of both materials showed a strong peak at 210 nm and the calculated optical band gaps were in the range of 4.72-4.92 eV.

Keywords: high energy milling, ball-to-powder weight ratio, XRD, TEM, UV-Vis

INTRODUCTION

SrWO₄ is an important member of alkaline-earth metal tungstate family with scheelite type structure where Sr ions are coordinated with eight oxygen atoms and W ions are connected to four oxygen atoms forming WO₄ groups [1]. This compound finds applications as: microwave dielectric material [2], host matrix for doping with rare earth active ions [3] anode material for lithium ion batteries [4], catalysts [5, 6], etc. Conventionally, SrWO₄ is prepared by the solid-state reaction of SrCO₃ and WO₃ between 700-1000 °C for several hours [7-9]. The sol-gel [4], hydrothermal synthesis [10], sonochemical method [11], co-precipitation [12], microwave-assisted route [13, 14], spark plasma sintering-reactive synthesis [15], electrochemical-assisted precipitation process [16] and mechanochemical synthesis [17] have been used for the preparation of this phase. The advantages of the mechanochemical method are: direct synthesis without additional heat treatment; decrease in synthesis time or temperature needed to obtain the final products; control of particle size and ability to prepare high purity materials like MOFs [18], inorganic mixed oxides [19, 20], etc. Many parameters as type of mill, milling speed, time, atmosphere or ball-to-powder weight ratio (BPR) affect the phase composition, microstructure, morphology and properties of the final products.

The major parameter during mechanochemical treatment is the milling speed which is a decisive factor for the rapid synthesis [19-23]. The high milling speed enables a faster synthesis while the low milling speed is not sufficient for completing the synthesis. The longer milling time may lead to the formation of undesirable phases [22, 24]. Types, size and number of balls used also play an important role in particle size of synthesized powders [25]. The BPR is another crucial parameter. The ratio has a significant effect on the time required to produce the desired phase or reduce the particle size. Generally, a higher value of this ratio will result in a shorter time required for phase formation [19]. The aim of the present work was to check the possibility for facile synthesis of SrWO₄ by mechanochemical activation using different ball-to-powder weight ratios (10:1 and 20:1). The formation of the desired phase, the morphology and optical properties of the obtained materials were discussed.

EXPERIMENTAL

A mixture of SrCO₃ (Merck, purity 99.9%) and WO₃ (Merck, purity 99.9%) in a molar ratio of 1:1 was subjected to intense mechanical treatment in a planetary ball mill (Fritsch–Premium line–Pulverisette No 7). Both vials and balls were made of stainless steel; the milling speed was 500 rpm.

* To whom all correspondence should be sent:
E-mail: m.gancheva@svr.igic.bas.bg

The ball-to-powder weight ratio (BPR) was 10:1 and 20:1. To minimize the temperature raise during the milling, the process was carried out for periods of 15 min, with rest periods of 5 min [26]. The milling process and the labels of samples are given in Table 1.

Table 1. The milling parameters of the mechanochemical process for preparation of SrWO₄

Sample	Milling speed	Ball-to-powder weight ratio (BPR)	Milling time
A	500 rpm	10:1	1-5h
B	500 rpm	20:1	1-3h

The phase and structural transformation of the milling samples were investigated by X-ray powder diffraction analysis (XRD) and infrared spectroscopy (IR). The powder X-ray diffraction study was performed on a Bruker D8 Advance instrument equipped with a copper tube (CuK α). The average crystallite sizes of SrWO₄ powders resulting from X-ray diffraction broadening were determined by the Scherrer's formula at the diffraction peak $2\theta = 33.10^\circ$. Infrared spectra were registered in the range of 1600–400 cm⁻¹ on a Nicolet-320 FTIR spectrometer using the KBr pellet technique. TEM observation was performed by a JEOL JEM-2100 microscope at an accelerating voltage of 200 kV. The preparation procedure of the specimen consisted of dispersing them in ethanol by ultrasonic treatment and dripping on standard Cu grids. UV-Vis spectra were recorded on an Evolution 300 spectrophotometer in the range from 200 to 1000 nm. The optical absorption band was calculated based on Tauc's equation $ah\nu = A(h\nu - E_g)^n$, where α is the absorption coefficient, A is the absorption constant, h is Planck's constant, ν is the photon frequency. In the mentioned relation, n represents the type of semiconductor charge transition [27]. The value of n is related to the characteristics of the electronic transition type in the semiconductors and $n = 0.5$ for a direct allowed transition; $n = 2$ for an indirect allowed transition; $n = 3$ for an indirect forbidden transition and $n = 3/2$ for a direct forbidden transition. SrWO₄ is known as a direct transition metal oxide, and therefore the value of $n = 0.5$ was selected to be used in Tauc's equation.

RESULTS AND DISCUSSION

The effect of the ball-to-powder weight ratio (BPR) on the formation of SrWO₄ powders was monitored by X-ray diffraction analysis (Figs. 1 and 2). Before ball milling the principal peaks of monoclinic WO₃ (PDF-01-043-1035) and orthorhombic SrCO₃ (PDF-00-005-0418) were observed.

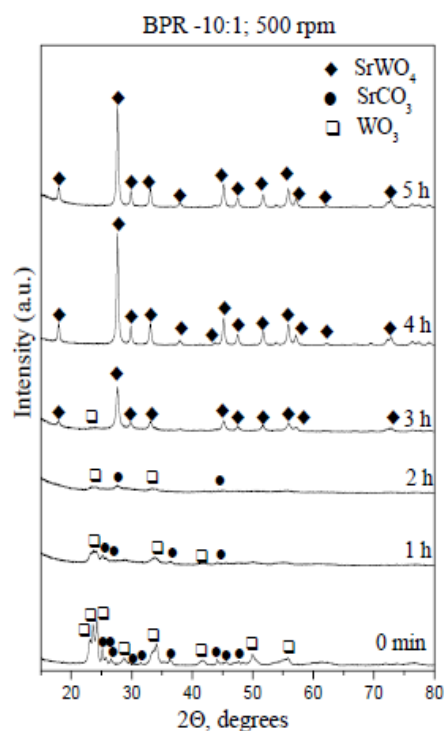


Fig. 1. XRD patterns of sample A mechanically activated for different milling times

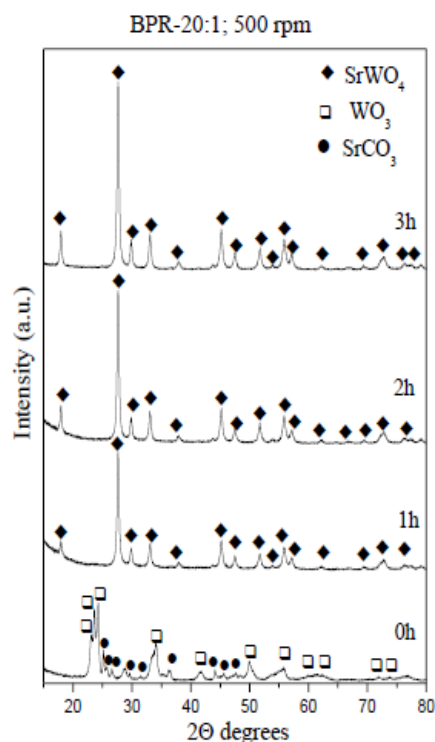


Fig. 2. XRD patterns of sample B mechanically activated for different milling times

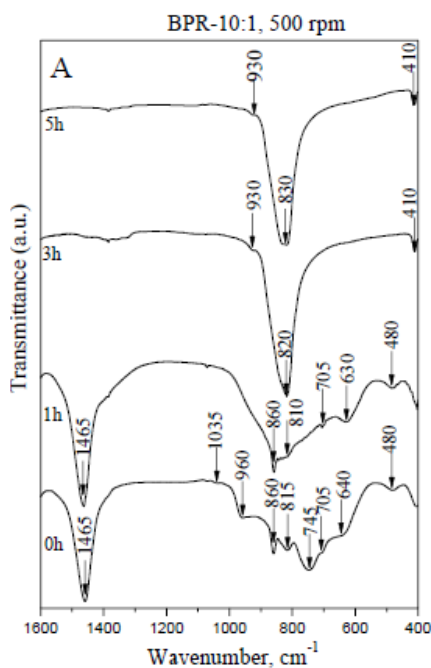


Fig. 3A. IR spectra of sample A mechanically activated for different milling times

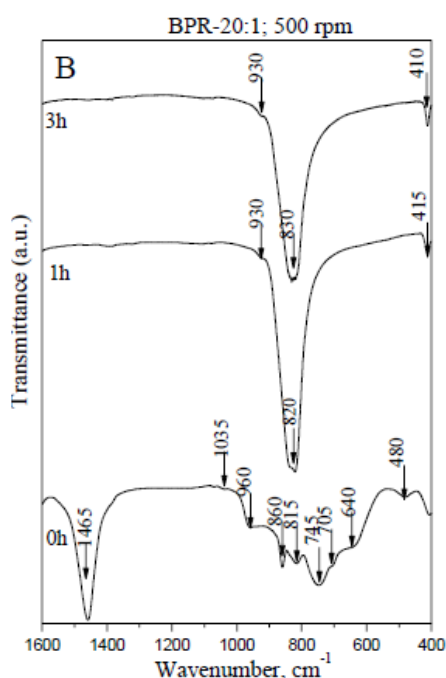


Fig. 3B. IR spectra of sample B mechanically activated for different milling times

After 1 h of milling time at a speed of 500 rpm using the lower BPR (10:1) they were broadened and their intensity had strongly decreased. This is a result of a reduction in particle sizes, destruction of the long-range order and accumulation of defects. During this milling process the initial reagents become amorphous. Increasing the milling time up to 3 h led to the appearance of new diffraction lines typical of the tetragonal type structure SrWO₄ (PDF-01-083-6135). The very low intensity peak at 23.70

° characteristic for WO₃ was also detected. The additional mechanochemical activation up to 4 h yielded a single phase of SrWO₄. Between 4 and 5 h of milling no change of XRD pattern was visible (Fig. 1).

The crystallite size of as-obtained SrWO₄ (after 5 h milling time) was calculated using Scherrer's equation for diffraction peak at $2\Theta = 33.10^\circ$ as 26 nm. With increasing BPR up to 20:1 at a milling speed of 500 rpm, the reaction between the reagents was performed after 1 h milling time (Fig. 2). Additional mechanical treatment up to 3 h did not lead to any changes in the XRD patterns of the sample. This is an indication for the structural stability of SrWO₄. The crystallite size of as-obtained SrWO₄ (after 1 h milling time) at the diffraction peak of $2\Theta = 33.10^\circ$ was 22 nm. The phase formation of SrWO₄ with increasing BPR (20:1) is due to the more effective solid-state diffusion between reagents in the course of ball-materials collisions.

The phase formation of SrWO₄ during the mechanochemical treatment was confirmed by IR spectroscopy. The IR spectrum of the non-activated mixture exhibits absorption bands typical of structural units of WO₃ (bands at 960, 815 and 745 cm⁻¹) and of SrCO₃ (bands at 1465, 860, 705 640 and 480 cm⁻¹) [28-30] (Figs. 3A and 3B). The IR spectra of the sample A activated at lower BPR (10:1) are presented in Fig. 3A. The bands at 1035, 960 and 745 cm⁻¹ disappeared after the early stages of the ball milling (1 h). Noticeable changes in the IR spectrum were observed after 3 h of milling time which confirmed the phase formation of SrWO₄. The new absorption bands are in good agreement with literature data [2, 11, 13, 14, 31]. The shoulder at 925 cm⁻¹ was assigned to anti-symmetry stretching vibrations (ν_1) in [WO₄] tetrahedral units. The strong band at 830 cm⁻¹ was attributed to the symmetry stretching vibration ν_3 of the same groups. The weak band at 410 cm⁻¹ is due to bending mode of the WO₄ entity [31]. For the material obtained using higher BPR (20:1) these bands appeared after 1 h of milling time indicating a faster chemical reaction (Fig. 3B).

The morphology and particle size distribution of SrWO₄ nanoparticles were analyzed by transmission electron microscopy. The TEM image at a lower magnification of the sample A shows that SrWO₄ nanocrystallites are aggregates consisting of many particles with nearly spherical form (Fig. 4A). The TEM images indicated that the particles exhibited homogeneity in shape (Figs. 4A and 4B). The particle size distribution histogram of sample A shown in Fig. 4C indicates that the grain sizes are between 10-60 nm and the average size is 21 nm.

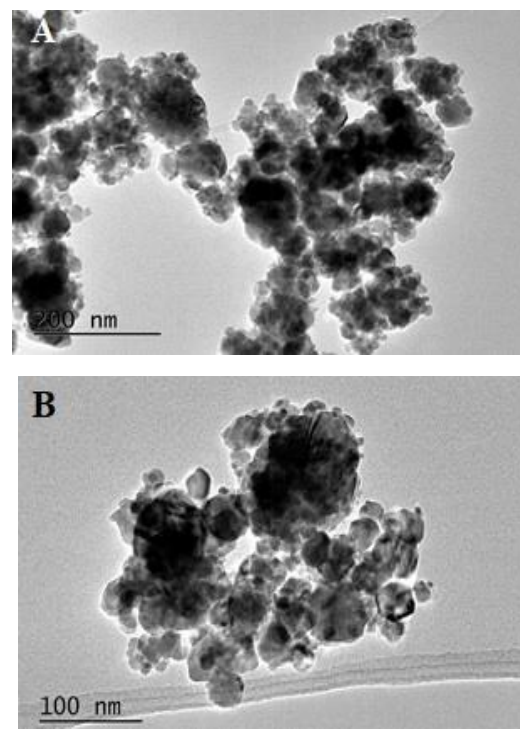
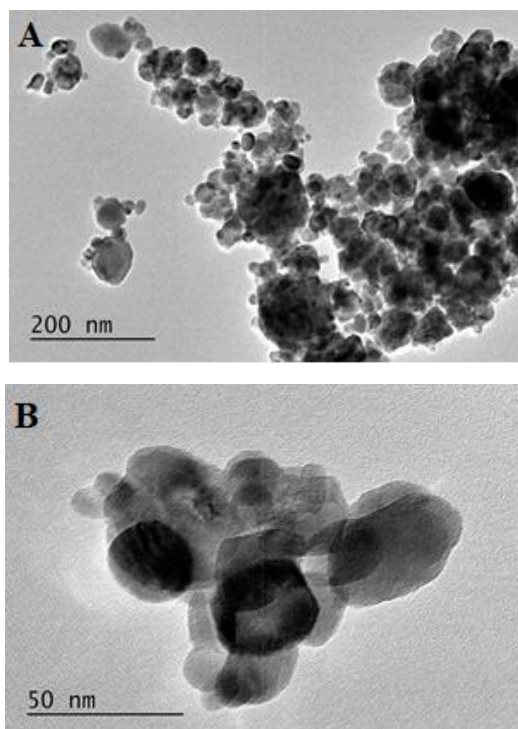


Fig. 4. TEM images (A and B) of the mechanochemically obtained SrWO₄ (sample A) after 5 h milling at BPR 10:1 and histogram of the particle size distribution (C).

The TEM studies of samples B (BPR 20:1) are presented in Fig. 5. No morphological differences were detected in SrWO₄ with the increase in BPR (Figs. 5A and 5B). In this case the crystallites exhibit more spherical form and their size is below 50 nm. With increasing BPR grain sizes between 1-40 nm were observed, the average size being 16 nm. The comparison of the particle size distribution of samples A and B shows that the particle size tends to decrease with the increase in BPR. The particle size distribution changed from narrow to wide from sample A to sample B.

Fig. 5. TEM images (A and B) of the mechanochemically obtained SrWO₄ (sample B) after 5 h milling at BPR 20:1 and histogram of the particle size distribution (C).

The optical properties of the mechanochemically obtained SrWO₄ powders were studied by UV-Vis diffuse reflectance spectroscopy. The UV-Vis reflectance spectra of SrWO₄ (samples A and B) exhibited a strong band at 210 nm which is typical for wide-band gap compounds (Fig. 6).

The peak at 210 nm is characteristic of O (2p) → W (5d) charge transfer in WO₄ tetrahedra [16]. The experimental optical band gap energy of nanocrystalline SrWO₄ was found by extrapolating the linear portion in an (F/R)^{1/2} vs. hv plot, as shown in Fig. 7.

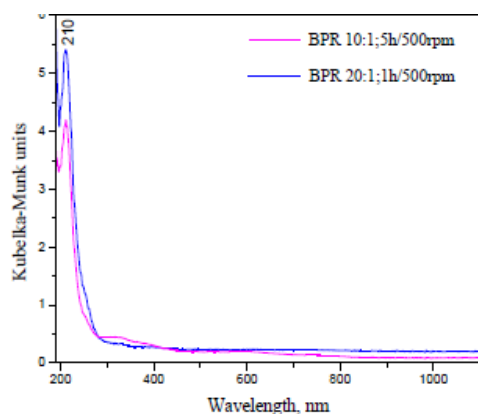


Fig. 6. Diffuse reflectance UV-Vis spectra of mechanochemically synthesized SrWO₄ powders at different BPR.

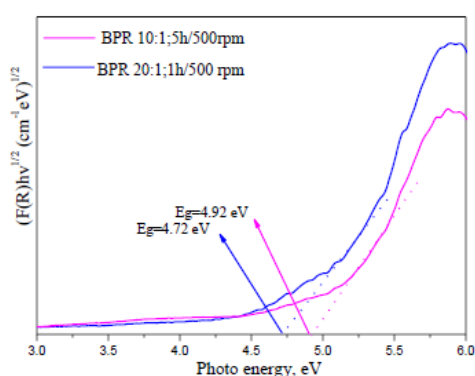


Fig. 7. Tauc plot of mechanochemically synthesized SrWO₄ powders at different BPR.

The band gap of the mechanochemically obtained SrWO₄ (sample A) was estimated to be 4.92 and decreased to 4.72 eV for SrWO₄ (sample B) using the higher ball-to-powder weight ratio 20:1. The value of the optical band gap is higher than those reported in the literature [3, 9, 16]. Table 2 gives the data of the average crystallite size and optical band gap value of both samples. The decrease in optical band gap value can be attributed to decreasing of the crystallite size.

Table 2. Mechanochemical synthesis of SrWO₄ and physico-chemical characteristics.

SrWO ₄	Milling time	D _{nm} ⁻ XRD	D _{nm} ⁻ TEM	E _g , eV
A	5 h BPR -10:1	27	22	4.92
B	1 h BPR -20:1	22	16	4.72

CONCLUSIONS

In this research, the effect of the ball-to-powder weight ratio (BPR) on the formation of SrWO₄ powder was studied. The mechanochemical treatment at lower BPR (10:1) and milling speed of 500 rpm induces amorphization of the reagents up to

2 h milling time. The phase formation of tetragonal SrWO₄ occurred at 5 h milling time. A faster synthesis of SrWO₄ was realized on applying a higher BPR (20:1) after 1 h of milling time with a milling speed of 500 rpm. The particle morphology of the as-obtained products mainly consists of special shapes. The average particle size determined by TEM analysis well matches that calculated from XRD data. UV-Vis spectroscopy indicated that SrWO₄ particles had strong visible light absorption and band gaps in the range of 4.72-4.92 eV.

Acknowledgements: The authors kindly acknowledge the financial support of project № BG05M2OP001-1.002-0014 „Centre of Competence HITMOBIL - Technologies and systems for generation, storage and consumption of clean energy”, funded by Operational Programme “Science and Education for Smart Growth” 2014-2020, co-funded by the EU from European Regional Development Fund.

REFERENCES

1. L. L. Chang, M. G. Scroger, B. Phillips, *J. Amer. Ceram. Soc.*, **49**, 385 (1966).
2. A. Priya, E. Sinha, S. K. Raou, *Solid State Science*, **20**, 40 (2013).
3. P. Jena, S. K. Gupta, K. Sudarshan, N. Pathak, A. K. Singh, *J. Mater. Sci.: Mater. Electron.*, **16** (2018)
4. L. Zhang, Q. Bai, L. Wang, A. Zhang, Y. Zhang, Y. Xing, *Func. Nat. Letters*, **7**, 1450010 (2014).
5. M. Kowalkinska, P. Gluchowski, T. Swebosci, T. Ossowski, A. Ossowski, W. Bednarski, J. Karcewski, A. Zielinska-Jurek, *J. Phys. Chem. C*, **125**, 25497 (2021).
6. M. Arunpandian, D. Sivaganesh, M. S. Revathy, K. Selvakumar, S. Arunachalam, D. Geetha, *Intern. J. Envir. Anal. Chem.*, (2020) doi: 10.1080/03067319.2020.1803847.
7. F. Jiandong, Z. Huaijin, W. Zhengping, G. Wenwei, W. Jiyang, *Front. Chem. China*, **3**, 264 (2006).
8. A. Afif, J. Zaini, S. M. H. Rahman, S. Eriksson, M. Aminul Islam, A. K. Azad, *Science Report*, **9**, 9173 (2019).
9. D. W. Kim, I. Cho, S. S. Shin, S. Lee, T. H. Noh, D. H. Kim, H. S. Jung, K. S. Hong, *J. Solid State Chem.*, **184**, 2103 (2011).
10. H. Pan, M. Hojamberdiev, G. Zhu, *J. Mater. Sci.*, **47**, 746 (2012).
11. T. Thongtem, A. Phuruangrat, S. Thongtem, *Appl. Surface Science*, **254**, 7581 (2008)
12. M. Muralidharan, V. Anbarasu, A. Elaya Perumal, K. Sivakumar, *J. Mater. Sci.: Mater. Electron.*, (2015).
13. C. S. Lim, *Asian J. Chem.*, **24**, 2843 (2021).
14. T. Thongtem, A. Phuruangrat, S. Thongtem, *J. Nanopart. Res.*, **12**, 2287 (2010).
15. E. K. Papyonov, O. O. Shichalin, I. Yu. Buravlev, A. A. Belov, A. S. Portnyagin, A. N. Fedorets, Yu. A.

- Azarova, I. G. Tananaev, V. I. Sergienko, *Vacuum*, **180**, 109628 (2020).
16. X. Li, Z. Song, B. Qu, *Ceram. Intern.*, **40**, 1205 (2014).
 17. L. Cheng, P. Liu, S. X. Qu, H. W. Zhang, *J. Alloys Comp.*, **581**, 553 (2013).
 18. A. P. Amrute, B. Zibrowius, F. Schüth, *Chem. Mater.*, **32**, 4699 (2020).
 19. M. Mancheva, R. Iordanova, Y. Dimitriev, *J. Alloys Compd.*, **509**, 15 (2011).
 20. M. Gancheva, T. Rojac, R. Iordanova, I. Piroeva, P. Ivanov, *Ceram. Intern.*, **48**, 17149 (2022).
 21. F. Palazon, Y. El Ajjouri, P. Sebastia-Luna, S. Lauciello, L. Manna, H. J. Bolink, *J. Mater. Chem. C*, **7**, 11406 (2019).
 22. C. Suryanarayana, *Intermetallics*, **3**, 153 (1995).
 23. S. Hwang, S. Grätz, L. Borchardt, *Chem. Commun.*, **58**, 1661 (2022).
 24. V. V. Boldyrev, *Russ. Chem. Rev.*, **75**, 203 (2006).
 25. M. Zakeria, M. Ramezani, A. Nazari, *Materials Research*, **15**, 891 (2012).
 26. M. Gancheva, R. Iordanova, Y. Dimitriev, D. Nihtianova, P. Stefanov, A. Naydenov, *J. Alloys Comp.*, **570**, 34 (2013).
 27. J. Tauc, *Mater. Res. Bull.*, **5**, 721 (1970).
 28. M. F. Daniel, B. Desbat, J. C. Lassegues, B. Gerand, M. Figlarz, *J. Solid State Chem.*, **67**, 235 (1987).
 29. C. L. Veenas, L. R. Asitha, V. C. Bose, A. S. A. Raj, G. Madhu, V. Biju, *Mater. Sci. Eng.*, **73**, 012119 (2015).
 30. P. Lu, X. Hu, Y. Li, M. Zhang, X. Liu, Y. He, F. Dong, M. Fub, Z. Zhan, *RSC Adv.*, **8**, 6315 (2018).
 31. G. M. Clark, W. P. Doyle, *Spectrochim. Acta*, **22**, 1441 (1966).